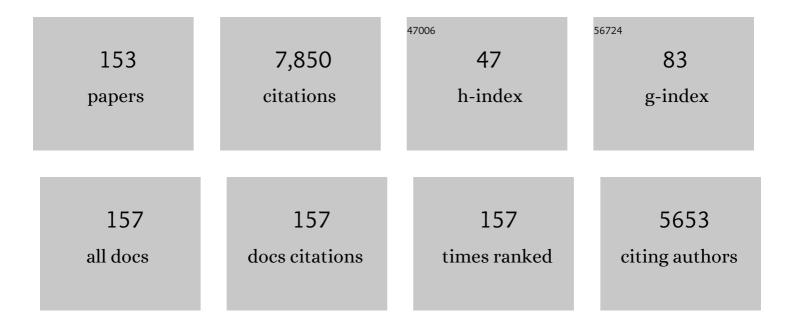
List of Publications by Year in descending order

Source: https://exaly.com/author-pdf/5873970/publications.pdf Version: 2024-02-01



#	Article	IF	CITATIONS
1	One-pot synthesis of highly dispersed mesoporous Cu/ZrO2 catalysts for NH3-SCR. Catalysis Today, 2022, 384-386, 113-121.	4.4	13
2	Effect of an Al2O3-based binder on the structure of extruded Fe-ZSM-5. Catalysis Today, 2022, 387, 207-215.	4.4	2
3	Experimental and modeling-based analysis of reaction pathways on catalysts for natural gas engines under periodic lean/rich oscillations. Chemical Engineering Journal, 2022, 430, 132848.	12.7	2
4	Restructuring Ni/Al2O3 by addition of Ga to shift product selectivity in CO2 hydrogenation: The role of hydroxyl groups. Journal of CO2 Utilization, 2022, 57, 101881.	6.8	6
5	Interconversion between Lewis and BrĄ̃nsted–Lowry acid sites on vanadia-based catalysts. Physical Chemistry Chemical Physics, 2022, 24, 4555-4561.	2.8	6
6	Redox Dynamics of Active VO <i>_x</i> Sites Promoted by TiO <i>_x</i> during Oxidative Dehydrogenation of Ethanol Detected by <i>Operando</i> Quick XAS. Jacs Au, 2022, 2, 762-776.	7.9	14
7	Investigation on the Role of Pd, Pt, Rh in Methane Abatement for Heavy Duty Applications. Catalysts, 2022, 12, 373.	3.5	4
8	<i>In situ</i> spectroscopic studies of the effect of water on the redox cycle of Cu ions in Cu-SSZ-13 during selective catalytic reduction of NO _{<i>x</i>} . Chemical Communications, 2022, 58, 6610-6613.	4.1	12
9	Poisoning of Mn-Ce/AC catalysts for low-temperature NH3-SCR of NO by K+ and its counter-ions (Clâ^'/NO3â^'/SO42â^'). Applied Catalysis A: General, 2022, 638, 118636.	4.3	11
10	In Situ Infrared Spectroscopy of NO _{<i>x</i>} Reduction Catalysts: A Laboratory Exercise for In-Person and Virtual Learning. Journal of Chemical Education, 2022, 99, 2649-2655.	2.3	3
11	Flexible application of biogas upgrading membranes for hydrogen recycle in power-to-methane processes. Chemical Engineering Science, 2021, 229, 116012.	3.8	24
12	HCN production from formaldehyde during the selective catalytic reduction of NOx with NH3 over V2O5/WO3-TiO2. Applied Catalysis B: Environmental, 2021, 281, 119462.	20.2	21
13	Effect of Short Reducing Pulses on the Dynamic Structure, Activity, and Stability of Pd/Al ₂ O ₃ for Wet Lean Methane Oxidation. ACS Catalysis, 2021, 11, 4870-4879.	11.2	19
14	Stable Palladium Oxide Clusters Encapsulated in Silicalite-1 for Complete Methane Oxidation. ACS Catalysis, 2021, 11, 7371-7382.	11.2	34
15	Grafting of Alkali Metals on Fumed Silica for the Catalytic Dehydrogenation of Methanol to Formaldehyde. ChemCatChem, 2021, 13, 3864-3877.	3.7	1
16	Reduction of PdO/Al ₂ O ₃ in Liquid Cyclohexane Followed <i>In Situ</i> by ATR-IR, High-Energy XRD, and XAS. Journal of Physical Chemistry C, 2021, 125, 16473-16482.	3.1	7
17	On the relevance of P poisoning in real-world DOC aging. Applied Catalysis B: Environmental, 2021, 291, 120062.	20.2	9
18	Reaction pathways of methane abatement in Pd-Rh three-way catalyst in heavy duty applications: A combined approach based on exhaust analysis, model gas reactor and DRIFTS measurements. Chemical Engineering Journal, 2021, 422, 129932.	12.7	12

#	Article	IF	CITATIONS
19	Recent progress in syngas production via catalytic CO2 hydrogenation reaction. Applied Catalysis B: Environmental, 2021, 295, 120319.	20.2	110
20	Techno-economic assessment of bioethanol production from lignocellulose by consortium-based consolidated bioprocessing at industrial scale. New Biotechnology, 2021, 65, 53-60.	4.4	12
21	Understanding the impact of poison distribution on the performance of Diesel oxidation catalysts. Applied Catalysis B: Environmental, 2021, 299, 120684.	20.2	8
22	Operando diffuse reflectance infrared detection of cyanide intermediate species during the reaction of formaldehyde with ammonia over V2O5/WO3-TiO2. Applied Catalysis B: Environmental, 2021, 298, 120629.	20.2	8
23	Increasing the activity of the Cu/CuAl ₂ O ₄ /Al ₂ O ₃ catalyst for the RWGS through preserving the Cu ²⁺ ions. Chemical Communications, 2021, 57, 1153-1156.	4.1	17
24	Investigating active phase loss from supported ruthenium catalysts during supercritical water gasification. Catalysis Science and Technology, 2021, 11, 7431-7444.	4.1	10
25	Structure and performance of zeolite supported Pd for complete methane oxidation. Catalysis Today, 2021, 382, 3-12.	4.4	24
26	Increased nickel exsolution from LaFe0.8Ni0.2O3 perovskite-derived CO2 methanation catalysts through strontium doping. Applied Catalysis A: General, 2020, 590, 117328.	4.3	13
27	Detection of key transient Cu intermediates in SSZ-13 during NH ₃ -SCR deNO _x by modulation excitation IR spectroscopy. Chemical Science, 2020, 11, 447-455.	7.4	52
28	Selective Catalytic Reduction of NO with NH ₃ on Cuâ^'SSZâ€13: Deciphering the Low and Highâ€ŧemperature Rateâ€limiting Steps by Transient XAS Experiments. ChemCatChem, 2020, 12, 1429-1435.	3.7	39
29	Engineering the ZrO ₂ –Pd Interface for Selective CO ₂ Hydrogenation by Overcoating an Atomically Dispersed Pd Precatalyst. ACS Catalysis, 2020, 10, 12058-12070.	11.2	24
30	Water Inhibition of Oxymethylene Dimethyl Ether Synthesis over Zeolite H-Beta: A Combined Kinetic and <i>in Situ</i> ATR-IR Study. ACS Catalysis, 2020, 10, 8106-8119.	11.2	20
31	Essential role of oxygen vacancies of Cu-Al and Co-Al spinel oxides in their catalytic activity for the reverse water gas shift reaction. Applied Catalysis B: Environmental, 2020, 266, 118669.	20.2	56
32	Ruthenium on phosphorous-modified alumina as an effective and stable catalyst for catalytic transfer hydrogenation of furfural. RSC Advances, 2020, 10, 11507-11516.	3.6	15
33	Nature of Synergy between BrÃ,nsted and Lewis Acid Sites in Sn–Beta Zeolites for Polyoxymethylene Dimethyl Ethers Synthesis. ChemSusChem, 2019, 12, 4421-4431.	6.8	20
34	Design of a Reactor Cell for Modulated Excitation Raman and DiffuseÂReflectance Studies of Selective Catalytic Reduction Catalysts. Emission Control Science and Technology, 2019, 5, 307-316.	1.5	13
35	Prominent role of mesopore surface area and external acid sites for the synthesis of polyoxymethylene dimethyl ethers (OME) on a hierarchical H-ZSM-5 zeolite. Catalysis Science and Technology, 2019, 9, 366-376.	4.1	28
36	Design of Stable Palladium-Based Zeolite Catalysts for Complete Methane Oxidation by Postsynthesis Zeolite Modification. ACS Catalysis, 2019, 9, 2303-2312.	11.2	82

#	Article	IF	CITATIONS
37	Modulated Excitation Raman Spectroscopy of V ₂ O ₅ /TiO ₂ : Mechanistic Insights into the Selective Catalytic Reduction of NO with NH ₃ . ACS Catalysis, 2019, 9, 6814-6820.	11.2	56
38	Cu–Al Spinel as a Highly Active and Stable Catalyst for the Reverse Water Gas Shift Reaction. ACS Catalysis, 2019, 9, 6243-6251.	11.2	76
39	Insights into the Nature of the Active Sites of Tinâ€Montmorillonite for the Synthesis of Polyoxymethylene Dimethyl Ethers (OME). ChemCatChem, 2019, 11, 3010-3021.	3.7	9
40	Segregation of Nickel/Iron Bimetallic Particles from Lanthanum Doped Strontium Titanates to Improve Sulfur Stability of Solid Oxide Fuel Cell Anodes. Catalysts, 2019, 9, 332.	3.5	3
41	Mechanochemistry-assisted hydrolysis of softwood over stable sulfonated carbon catalysts in a semi-batch process. RSC Advances, 2019, 9, 33525-33538.	3.6	6
42	Sulfur Poisoning Recovery on a Solid Oxide Fuel Cell Anode Material through Reversible Segregation of Nickel. Chemistry of Materials, 2019, 31, 748-758.	6.7	36
43	Thermal activation and aging of a V2O5/WO3-TiO2 catalyst for the selective catalytic reduction of NO with NH3. Applied Catalysis A: General, 2019, 573, 64-72.	4.3	25
44	Mechanistic implications of lanthanum-modification on gold-catalyzed formic acid decomposition under SCR-relevant conditions. Applied Catalysis B: Environmental, 2019, 244, 709-718.	20.2	6
45	Effect of SiO2 on co-impregnated V2O5/WO3/TiO2 catalysts for the selective catalytic reduction of NO with NH3. Catalysis Today, 2019, 320, 123-132.	4.4	21
46	Time-resolved copper speciation during selective catalytic reduction of NO on Cu-SSZ-13. Nature Catalysis, 2018, 1, 221-227.	34.4	186
47	Methane oxidation over a honeycomb Pd-only three-way catalyst under static and periodic operation. Applied Catalysis B: Environmental, 2018, 220, 67-77.	20.2	67
48	Mitigation of Secondary Organic Aerosol Formation from Log Wood Burning Emissions by Catalytic Removal of Aromatic Hydrocarbons. Environmental Science & Technology, 2018, 52, 13381-13390.	10.0	10
49	Selective Catalytic Reduction of NOx. Catalysts, 2018, 8, 459.	3.5	22
50	Stable complete methane oxidation over palladium based zeolite catalysts. Nature Communications, 2018, 9, 2545.	12.8	187
51	Numerical Modeling of Hydroperoxyl-Mediated Oxidative Dehydrogenation of Formic Acid under SCR-Relevant Conditions. Industrial & Engineering Chemistry Research, 2018, 57, 10206-10215.	3.7	0
52	Deactivation and Regeneration of Sulfonated Carbon Catalysts in Hydrothermal Reaction Environments. ChemSusChem, 2018, 11, 2189-2201.	6.8	33
53	Impact of Catalyst Geometry on Diffusion and Selective Catalytic Reduction Kinetics under Elevated Pressures. Chemie-Ingenieur-Technik, 2018, 90, 795-802.	0.8	2
54	Selective synthesis of dimethyl ether on eco-friendly K10 montmorillonite clay. Applied Catalysis A: General, 2018, 560, 165-170.	4.3	14

#	Article	IF	CITATIONS
55	Reversible Segregation of Ni in LaFe 0.8 Ni 0.2 O 3± δ During Coke Removal. ChemCatChem, 2018, 10, 4456-4464.	3.7	15
56	Increasing the Sensitivity to Short-Lived Species in a Modulated Excitation Experiment. Analytical Chemistry, 2017, 89, 5801-5809.	6.5	21
57	High energy X-ray diffraction and IR spectroscopy of Pt/Al2O3 during CO oxidation in a novel catalytic reactor cell. Journal of Lithic Studies, 2017, 3, 71-78.	0.5	17
58	Catalytic synthesis of polyoxymethylene dimethyl ethers (OME): A review. Applied Catalysis B: Environmental, 2017, 217, 407-420.	20.2	148
59	Water-assisted oxygen activation during gold-catalyzed formic acid decomposition under SCR-relevant conditions. Journal of Catalysis, 2017, 349, 197-207.	6.2	11
60	Structural Reversibility and Nickel Particle stability in Lanthanum Iron Nickel Perovskiteâ€₹ype Catalysts. ChemSusChem, 2017, 10, 2505-2517.	6.8	52
61	Relationship between structures and activities of supported metal vanadates for the selective catalytic reduction of NO by NH3. Applied Catalysis B: Environmental, 2017, 218, 731-742.	20.2	72
62	Deactivation Aspects of Methane Oxidation Catalysts Based on Palladium and ZSM-5. Topics in Catalysis, 2017, 60, 123-130.	2.8	34
63	Operando XAS study of the influence of CO and NO on methane oxidation by Pd/Al ₂ O ₃ . Journal of Physics: Conference Series, 2016, 712, 012051.	0.4	4
64	The Significance of Lewis Acid Sites for the Selective Catalytic Reduction of Nitric Oxide on Vanadiumâ€Based Catalysts. Angewandte Chemie, 2016, 128, 12168-12173.	2.0	22
65	Understanding the anomalous behavior of Vegard's law in Ce _{1â^x} M _x O ₂ (M = Sn and Ti; 0 < x ≤0.5) solid solutions. Physical Chemistry Chemical Physics, 2016, 18, 13974-13983.	2.8	21
66	An operando emission spectroscopy study of Pt/Al ₂ O ₃ and Pt/CeO ₂ /Al ₂ O ₃ . Physical Chemistry Chemical Physics, 2016, 18, 29268-29277.	2.8	12
67	The Significance of Lewis Acid Sites for the Selective Catalytic Reduction of Nitric Oxide on Vanadiumâ€Based Catalysts. Angewandte Chemie - International Edition, 2016, 55, 11989-11994.	13.8	228
68	Selectivity Control in Palladium-Catalyzed Alcohol Oxidation through Selective Blocking of Active Sites. Journal of Physical Chemistry C, 2016, 120, 14027-14033.	3.1	50
69	Measurement of Vanadium Emissions from SCR Catalysts by ICP-OES: Method Development and First Results. Emission Control Science and Technology, 2015, 1, 292-297.	1.5	7
70	Structural Modification of Ni/γâ€Al ₂ O ₃ with Boron for Enhanced Carbon Resistance during CO Methanation. ChemCatChem, 2015, 7, 3261-3265.	3.7	11
71	Operando Attenuated Total Reflectance FTIR Spectroscopy: Studies on the Different Selectivity Observed in Benzyl Alcohol Oxidation. ChemCatChem, 2015, 7, 2534-2541.	3.7	23
72	VOx Surface Coverage Optimization of V2O5/WO3-TiO2 SCR Catalysts by Variation of the V Loading and by Aging. Catalysts, 2015, 5, 1704-1720.	3.5	82

#	Article	IF	CITATIONS
73	Generation of NH ₃ Selective Catalytic Reduction Active Catalysts from Decomposition of Supported FeVO ₄ . ACS Catalysis, 2015, 5, 4180-4188.	11.2	64
74	CO Methanation for Synthetic Natural Gas Production. Chimia, 2015, 69, 608.	0.6	15
75	Promotion of Ammonium Formate and Formic Acid Decomposition over Au/TiO2 by Support Basicity under SCR-Relevant Conditions. ACS Catalysis, 2015, 5, 4772-4782.	11.2	15
76	WOâ,ƒ/CeOâ,,/TiOâ,, Catalysts for Selective Catalytic Reduction of NOx by NHâ,ƒ: Effect of the Synthesis Method. Chimia, 2015, 69, 220.	0.6	12
77	Comparative analysis on the performance of pressure and air-assisted urea injection for selective catalytic reduction of NOx. Fuel, 2015, 161, 269-277.	6.4	40
78	Flame-Made WO ₃ /CeO _{<i>x</i>} -TiO ₂ Catalysts for Selective Catalytic Reduction of NO _{<i>x</i>} by NH ₃ . ACS Catalysis, 2015, 5, 5657-5672.	11.2	171
79	Ammonia Storage and Release in SCR Systems for Mobile Applications. Fundamental and Applied Catalysis, 2014, , 485-506.	0.9	6
80	Pre-Turbo Scr - Influence of Pressure on NOx Reduction. MTZ Worldwide, 2014, 75, 46-51.	0.1	11
81	Ammonium formate decomposition over Au/TiO ₂ : a unique case of preferential selectivity against NH ₃ oxidation. Chemical Communications, 2014, 50, 6998-7000.	4.1	6
82	Effect of ammonia on the decomposition of ammonium formate over Au/TiO 2 under oxidizing conditions relevant to SCR: Enhancement of formic acid decomposition rate and CO 2 production. Applied Catalysis A: General, 2014, 486, 219-229.	4.3	14
83	Liquid-Phase Catalytic Decomposition of Novel Ammonia Precursor Solutions for the Selective Catalytic Reduction of NOx. Topics in Catalysis, 2013, 56, 19-22.	2.8	4
84	Hydrothermally Stable WO3/ZrO2–Ce0.6Zr0.4O2 Catalyst for the Selective Catalytic Reduction of NO with NH3. Topics in Catalysis, 2013, 56, 23-28.	2.8	9
85	Diesel Soot Catalyzes the Selective Catalytic Reduction of NOx with NH3. Topics in Catalysis, 2013, 56, 440-445.	2.8	3
86	Theoretical studies of HNCO adsorption at stabilized iron complexes in the ZSM-5 framework. Microporous and Mesoporous Materials, 2013, 169, 97-102.	4.4	10
87	Adsorption and catalytic thermolysis of gaseous urea on anatase TiO2 studied by HPLC analysis, DRIFT spectroscopy and DFT calculations. Applied Catalysis B: Environmental, 2013, 134-135, 316-323.	20.2	30
88	Catalytic urea hydrolysis in the selective catalytic reduction of NO _x : catalyst screening and kinetics on anatase TiO ₂ and ZrO ₂ . Catalysis Science and Technology, 2013, 3, 942-951.	4.1	64
89	Quantification of Gaseous Urea by FT-IR Spectroscopy and Its Application in Catalytic Urea Thermolysis. Topics in Catalysis, 2013, 56, 130-133.	2.8	13
90	DRIFTS studies on CO and NO adsorption and NO+CO reaction over Pd2+-substituted CeO2 and Ce0.75Sn0.25O2 catalysts. Journal of Catalysis, 2013, 303, 117-129.	6.2	67

#	Article	IF	CITATIONS
91	Subsecond and in Situ Chemical Speciation of Pt/Al ₂ O ₃ during Oxidation–Reduction Cycles Monitored by High-Energy Resolution Off-Resonant X-ray Spectroscopy. Journal of the American Chemical Society, 2013, 135, 19071-19074.	13.7	43
92	Calibration of a model for selective catalytic reduction with ammonia, including NO oxidation, and simulation of NO _x reduction over an Fe–zeolite catalyst under highly transient conditions. International Journal of Engine Research, 2013, 14, 107-121.	2.3	6
93	Harnstoffhydrolyse für die selektive katalytische Reduktion von NOx: Vergleich der Flüssig- und Gasphasenzersetzung. Chemie-Ingenieur-Technik, 2013, 85, 625-631.	0.8	6
94	Active Sites, Deactivation and Stabilization of Fe-ZSM-5 for the Selective Catalytic Reduction (SCR) of NO with NH3. Chimia, 2012, 66, 687-693.	0.6	11
95	Selective Catalytic Reduction of Nitrogen Oxide — Part 1: Formates as Ammonia Storage Compounds. MTZ Worldwide, 2012, 73, 60-66.	0.1	2
96	Selective Catalytic Reduction of NO _{<i>x</i>} with Ammonia over Soot. ACS Catalysis, 2012, 2, 1507-1518.	11.2	24
97	The influence of H2SO4 on soot oxidation with NO2. Carbon, 2012, 50, 2100-2109.	10.3	9
98	Hydrolysis and thermolysis of urea and its decomposition byproducts biuret, cyanuric acid and melamine over anatase TiO2. Applied Catalysis B: Environmental, 2012, 115-116, 129-137.	20.2	135
99	Effect of Structural and Preparation Parameters on the Activity and Hydrothermal Stability of Metal-Exchanged ZSM-5 in the Selective Catalytic Reduction of NO by NH ₃ . Industrial & Engineering Chemistry Research, 2011, 50, 4308-4319.	3.7	50
100	Guanidinium Formate Decomposition on the (101) TiO ₂ -Anatase Surface: Combined Minimum Energy Reaction Pathway Calculations and Temperature-Programmed Decomposition Experiments. Journal of Physical Chemistry C, 2011, 115, 1195-1203.	3.1	12
101	Evaporation of Urea at Atmospheric Pressure. Journal of Physical Chemistry A, 2011, 115, 2581-2589.	2.5	48
102	Development of a TG-FTIR system for investigations with condensable and corrosive gases. Journal of Thermal Analysis and Calorimetry, 2011, 105, 545-552.	3.6	11
103	A Niobia-Ceria based multi-purpose catalyst for selective catalytic reduction of NOx, urea hydrolysis and soot oxidation in diesel exhaust. Applied Catalysis B: Environmental, 2011, 103, 79-84.	20.2	61
104	Hydrothermal deactivation of Fe-ZSM-5 catalysts for the selective catalytic reduction of NO with NH3. Applied Catalysis B: Environmental, 2011, 101, 649-659.	20.2	103
105	Laboratory test reactor for the investigation of liquid reducing agents in the selective catalytic reduction of NOx. Review of Scientific Instruments, 2011, 82, 084101.	1.3	25
106	The determination of the activities of different iron species in Fe-ZSM-5 for SCR of NO by NH3. Applied Catalysis B: Environmental, 2010, 95, 348-357.	20.2	199
107	Estimation of the fractions of different nuclear iron species in uniformly metal-exchanged Fe-ZSM-5 samples based on a Poisson distribution. Applied Catalysis A: General, 2010, 373, 168-175.	4.3	66
108	Characterization of Nb-Containing MnO _{<i>x</i>} â^'CeO ₂ Catalyst for Low-Temperature Selective Catalytic Reduction of NO with NH ₃ . Journal of Physical Chemistry C, 2010, 114, 9791-9801.	3.1	119

#	Article	IF	CITATIONS
109	The role of BrÃnsted acidity in the selective catalytic reduction of NO with ammonia over Fe-ZSM-5. Journal of Catalysis, 2009, 268, 297-306.	6.2	167
110	Materials for thermohydrolysis of urea in a fluidized bed. Chemical Engineering Journal, 2009, 152, 167-176.	12.7	17
111	Decomposition of Urea in the SCR Process: Combination of DFT Calculations and Experimental Results on the Catalytic Hydrolysis of Isocyanic Acid on TiO2 and Al2O3. Topics in Catalysis, 2009, 52, 1740-1745.	2.8	19
112	DFT study of structural and vibrational properties of guanidinium derivatives. Computational and Theoretical Chemistry, 2009, 907, 16-21.	1.5	15
113	Hydrolysis and oxidation of gaseous HCN over heterogeneous catalysts. Applied Catalysis B: Environmental, 2009, 92, 75-89.	20.2	100
114	A model gas study of ammonium formate, methanamide and guanidinium formate as alternative ammonia precursor compounds for the selective catalytic reduction of nitrogen oxides in diesel exhaust gas. Applied Catalysis B: Environmental, 2009, 88, 66-82.	20.2	59
115	Screening of doped MnO –CeO2 catalysts for low-temperature NO-SCR. Applied Catalysis B: Environmental, 2009, 88, 413-419.	20.2	237
116	Determination of Effective Diffusion Coefficients through the Walls of Coated Diesel Particulate Filters. Industrial & Engineering Chemistry Research, 2009, 48, 10746-10750.	3.7	11
117	Adsorption and Desorption of SO _{<i>x</i>} on Diesel Oxidation Catalysts. Industrial & Engineering Chemistry Research, 2009, 48, 9847-9857.	3.7	73
118	Modelling Catalyst Surfaces Using DFT Cluster Calculations. International Journal of Molecular Sciences, 2009, 10, 4310-4329.	4.1	30
119	DFT calculations, DRIFT spectroscopy and kinetic studies on the hydrolysis of isocyanic acid on the TiO2-anatase (101) surface. Journal of Molecular Catalysis A, 2008, 280, 68-80.	4.8	28
120	Chemical deactivation of V2O5/WO3–TiO2 SCR catalysts by additives and impurities from fuels, lubrication oils, and urea solution. Applied Catalysis B: Environmental, 2008, 77, 215-227.	20.2	184
121	Chemical deactivation of V2O5/WO3–TiO2 SCR catalysts by additives and impurities from fuels, lubrication oils and urea solution. Applied Catalysis B: Environmental, 2008, 77, 228-236.	20.2	243
122	The State of the Art in Selective Catalytic Reduction of NO _x by Ammonia Using Metalâ€Exchanged Zeolite Catalysts. Catalysis Reviews - Science and Engineering, 2008, 50, 492-531.	12.9	758
123	Combination of V ₂ O ₅ /WO ₃ â^`TiO ₂ , Feâ^`ZSM5, and Cuâ^`ZSM5 Catalysts for the Selective Catalytic Reduction of Nitric Oxide with Ammonia. Industrial & Engineering Chemistry Research, 2008, 47, 8588-8593.	3.7	59
124	Ammonia measurement with a pH electrode in the ammonia/urea-SCR process. Measurement Science and Technology, 2007, 18, 771-778.	2.6	3
125	Chapter 9 Aspects of catalyst development for mobile urea-SCR systems — From Vanadia-Titania catalysts to metal-exchanged zeolites. Studies in Surface Science and Catalysis, 2007, 171, 261-289.	1.5	38
126	Basic investigation of the chemical deactivation of V2O5/WO3-TiO2 SCR catalysts by potassium, calcium, and phosphate. Topics in Catalysis, 2007, 42-43, 333-336.	2.8	50

#	Article	IF	CITATIONS
127	Investigation of HNCO adsorption and hydrolysis on Fe-ZSM5. Catalysis Letters, 2007, 115, 33-39.	2.6	32
128	Characterization and catalytic investigation of Fe-ZSM5 for urea-SCR. Catalysis Today, 2007, 119, 137-144.	4.4	135
129	Isocyanic acid hydrolysis over Fe-ZSM5 in urea-SCR. Catalysis Communications, 2006, 7, 600-603.	3.3	59
130	DFT modeling of the hydrolysis of isocyanic acid over the TiO2 anatase (101) surface: Adsorption of HNCO species. Surface Science, 2006, 600, 5158-5167.	1.9	20
131	Influence of Potassium Doping on the Activity and the Sulfur Poisoning Resistance of Soot Oxidation Catalysts. Catalysis Letters, 2006, 109, 49-53.	2.6	20
132	MnOx-CeO2 mixed oxides for the low-temperature oxidation of diesel soot. Applied Catalysis B: Environmental, 2006, 64, 72-78.	20.2	160
133	Adsorption and hydrolysis of isocyanic acid on TiO2. Applied Catalysis B: Environmental, 2006, 65, 55-61.	20.2	50
134	Influence of NO2 on the hydrolysis of isocyanic acid over TiO2. Applied Catalysis B: Environmental, 2006, 65, 169-174.	20.2	32
135	Investigation of the selective catalytic reduction of NO by NH3 on Fe-ZSM5 monolith catalysts. Applied Catalysis B: Environmental, 2006, 66, 208-216.	20.2	176
136	Manganese based materials for diesel exhaust SO2 traps. Applied Catalysis B: Environmental, 2006, 67, 160-167.	20.2	27
137	Influence of NO2 on the selective catalytic reduction of NO with ammonia over Fe-ZSM5. Applied Catalysis B: Environmental, 2006, 67, 187-196.	20.2	282
138	An ammonia and isocyanic acid measuring method for soot containing exhaust gases. Analytica Chimica Acta, 2005, 537, 393-400.	5.4	29
139	Catalytic investigation of Fe-ZSM5 in the selective catalytic reduction of NOxwith NH3. Reaction Kinetics and Catalysis Letters, 2005, 86, 347-354.	0.6	38
140	Catalytic oxidation of nitrogen monoxide over Pt/SiO2. Applied Catalysis B: Environmental, 2004, 50, 73-82.	20.2	205
141	Storage of NO2 on BaO/TiO2 and the influence of NO. Applied Catalysis B: Environmental, 2003, 43, 389-395.	20.2	45
142	Adsorption and desorption of NO and NO2 on Cu-ZSM-5. Microporous and Mesoporous Materials, 2003, 58, 175-183.	4.4	66
143	Catalytic Wall Reactor as a Tool for Isothermal Investigations in the Heterogeneously Catalyzed Oxidation of Propene to Acrolein. Industrial & Engineering Chemistry Research, 2002, 41, 1445-1453.	3.7	41
144	Silica xerogels containing bidentate phosphine ruthenium complexes: textural properties and catalytic behaviour in the synthesis of N,N-dimethylformamide from carbon dioxide. Microporous and Mesoporous Materials, 2000, 35-36, 181-193.	4.4	25

#	Article	IF	CITATIONS
145	Silica hybrid gel catalysts containing ruthenium complexes: influence of reaction parameters on the catalytic behaviour in the synthesis of N,N-dimethylformamide from carbon dioxide. Journal of Molecular Catalysis A, 1999, 140, 185-193.	4.8	35
146	Silica Hybrid Gel Catalysts Containing Group(VIII) Transition Metal Complexes: Preparation, Structural, and Catalytic Properties in the Synthesis ofN,N-Dimethylformamide and Methyl Formate from Supercritical Carbon Dioxide. Journal of Catalysis, 1998, 178, 284-298.	6.2	180
147	Highly active ruthenium complexes with bidentate phosphine ligands for the solvent-free catalytic synthesis of N,N-dimethylformamide and methyl formate. Chemical Communications, 1997, , 453-454.	4.1	145
148	Sol–gel derived hybrid materials as heterogeneous catalysts for the synthesis of N,N-dimethylformamide from supercritical carbon dioxide. Chemical Communications, 1996, , 1497-1498.	4.1	67
149	Synthesis of N,N-dimethylformamide by heterogeneous catalytic hydrogenation of supercritical carbon dioxide. Process Technol, 1996, , 91-96.	0.1	10
150	Synthesis and absolute stereostructure of dinaphth[2,1- c: 1′,2′-e]oxepin-3-(5H)-one. Tetrahedron, 1994, 50, 2831-2840.	1.9	15
151	Transient simulation of NO _x reduction over a Fe-Zeolite catalyst in an NH ₃ -SCR system and study of the performance under different operating conditions. SAE International Journal of Fuels and Lubricants, 0, 5, 370-379.	0.2	14
152	Acidic Zirconia Mixed Oxides for NH ₃ -SCR Catalysts for PC and HD Applications. , 0, , .		12
153	Development of a 3rd Generation SCR NH ₃ -Direct Dosing System for Highly Efficient DeNOx. SAE International Journal of Engines, 0, 5, 938-946.	0.4	15